Mathematical Biosciences and Engineering

MBE, 19(6): 5591–5609.
DOI: 10.3934/mbe.2022262
Received: 08 December 2021
Revised: 21 February 2022
Accepted: 07 March 2022
Published: 30 March 2022

http://www.aimspress.com/journal/MBE

Research article

Design of generalized fault diagnosis observer and active adaptive fault tolerant controller for aircraft control system

Rong Sun, Yuntao Han* and Yingying Wang*

College of Intelligent Systems Science and Engineering, Harbin Engineering University, Harbin 150001, China

* **Correspondence:** Email: yuntaohan @163.com, w_winny@hrbeu.edu.cn.

Abstract: This study aims to design a generalized fault diagnosis observer (GFDO) and an active fault tolerant control system (AFTCS) for external disturbances based on an aircraft control system and actuator faults. Unlike the traditional approach that assumes external disturbances are norm bounded, the Gronwall Lemma based on the external disturbances constraint condition is modelled to satisfy the system stability. Then, the GFDO is designed by two performance indices defined to simultaneously estimate system states and faults. In addition, the AFTCS is designed to obtain the desired performances in the fault case. When the fault is diagnosed by GFDO, the regular controller switches to AFTCS. Finally, an analysis of the performance of the proposed algorithm is discussed based on simulations of the F-18 aircraft control system, which illustrates the effectiveness and applicability of this method.

Keywords: fault estimation; fault tolerant control; actuator fault; aircraft control system

1. Introduction

Actuator failures may cause serious performance deterioration of plant control systems or lead to systems divergence and catastrophic accidents. Fault diagnosis and fault tolerant control (FTC) algorithms for actuator failures are adaptable in the sense that the presence of sensor faults can be easily handled by recasting them as actuator faults. Therefore, most existing research results have focused on actuator failures [1–4]. Reference [1] reviewed the current state of the art on spacecraft attitude FTC design. The existing approaches for FTC can be categorized as fault management approaches in engineering, model-based fault detection and diagnosis (FDD), and data-driven-based FDD. The paper reviewed the recent spacecraft attitude FTC design methods and concluded that each approach had its own advantages and limitations. A primary goal for fault estimation and fault tolerant control algorithm design is to maintain the systems stability or desired performance in the presence of faults, especially in safety-critical systems, such as the aircraft control system. The fault of the aircraft control system can be characterized by hierarchy and correlativity; in other words, system breakdown or even personal injury can be induced by a fault. As a result, a considerable amount of research on fault diagnosis for aircraft control systems has been reported in the literature [5–9].

A number of approaches to the design of fault tolerant control systems (FTCSs) have been published. These methods can be broadly classified into passive FTCSs (PFTCSs) [10–12] and active FTCSs (AFTCSs). In [3], PFTCS and AFTCS were analysed and their fundamental components were compared from the theoretical perspective which highlighted their advantages and disadvantages. The PFTCS is designed off-line and does not access fault information on-line and only performs effectively for the presumed faults. In contrast, the AFTCS considers some limitations. In the AFTCS, the fault estimation is considered and then the fault tolerant controller synthesized online from the estimated fault information estimated is constructed. Therefore, the AFTCS methods satisfy the reliability and stability requirements for the aircraft control system. An AFTCS approach offers more efficiency than PFTCSs with different types of faults. However, the controller performance is primarily dependent on its fault detection and isolation unit for providing timely and accurate fault information. Generally, the AFTCS includes learning-based approaches [13–16], full state constraints [17], high-gain observers [18], unknown input observers [19,20], robust control [2,12,21–24], sliding mode control [25,26] and adaptive control strategies [11,12,27–30]. In [31], a robust adaptive fault diagnosis observer was proposed for a nonlinear aircraft system with actuator faults and external disturbances. The designed observer exhibits robustness to the disturbances and is sensitive to the actuator faults to be detected. However, the supremum of external disturbances is a constant selected at random, as described in [31]. Most of the existing research dealt with the constraint condition of the external disturbances, as shown in [31], for example, [27]. As a result, we examine the constraint condition that satisfies the system stability in this paper. In [12,32], it was assumed that the faults to be detected are known a prior. In [33], a robust hybrid observer for a switched linear system with a prior known fault was designed, and then the optimal trade-off algorithm between robustness to external disturbances and sensitivity to faults was realized by the LMI procedure. Fault estimation in the process of fault diagnosis can improve false alarm rates. Therefore, presenting an observer that can estimate the fault and states simultaneously is beneficial for the abovementioned fault-tolerant control design. In [7,34], the authors provided the state feedback and output feedback fault tolerant controller with constant gain matrices. The performance and precision of fault-tolerant controllers for systems are governed by the constant gain matrices of the FTC. However, the performance of FTC is not ensured by the constant gain. Therefore, the design of AFTCSs is crucial for the high performance demands in military applications, such as aircraft control systems.

The main contributions of this paper are as follows. Our work was motivated by the limitations of the references mentioned above, unlike [27,35] we do not assume that the constraint condition of external disturbances was known as a priori or even norm bounded, for example, $\|g(\cdot)\| \leq 6$. Instead, a novel constraint condition that satisfies the system stability requirement is derived in this paper. This is the first study to research the external disturbance constraint condition under the design of AFTCS background. Moreover, a generalized fault diagnosis observer that can estimate the states and fault simultaneously based on Lyapunov stability theory by resorting to the external disturbance information derived previously is proposed. To obtain the desired performance fault-tolerant controller, the AFTCS, which can adaptively adjust controller parameters and compensate for the fault and external disturbances, is used. Furthermore, the proposed algorithm guarantees asymptotical convergence of the states.

The rest of this paper is organized as follows. The problem and preliminary lemma are briefly introduced in Section 2. The external disturbances of the system are analysed in Section 3. The fault estimation algorithm is discussed in Section 4. Some main results of the active adaptive fault tolerant control design method are proposed in Section 5. An aircraft control example is used to verify the effectiveness of the proposed algorithm in Section 6. Finally, conclusions are drawn in Section 7.

Notations. For a given matrix $\boldsymbol{A}$, $\boldsymbol{A}^T$ denotes its transpose. $\boldsymbol{I}$ denotes the identity matrix with appropriate dimensions. $\|\cdot\|$ represents the Euclidean norm of vectors or matrices. $\lambda_{\min}(\cdot)$ and $\lambda_{\max}(\cdot)$ denote the minimum and maximum eigenvalues of matrix $(\cdot)$, respectively.

2. Preliminaries and problem statement

The system discussed in this research can be described as (1), which is a linear system with actuator faults and external disturbances.

$$\dot{\boldsymbol{x}}(t) = \boldsymbol{A}\boldsymbol{x}(t) + \boldsymbol{B}\boldsymbol{u}(t) + \boldsymbol{D}_1\boldsymbol{d}(t) + \boldsymbol{R}\boldsymbol{f}(t) \tag{1}$$

$$\boldsymbol{y}(t) = \boldsymbol{C}\boldsymbol{x}(t) + \boldsymbol{D}_2\boldsymbol{d}(t) \tag{2}$$

where $\boldsymbol{x}(t)$ represents the state vector, $\boldsymbol{u}(t)$ and $\boldsymbol{y}(t)$ are the control input vector and the measured output vector, respectively. $\boldsymbol{d}(t)$ represents the external disturbance vector. The external disturbance vector can also be considered as the unmodelled errors and modelling uncertainties. $\boldsymbol{f}(t)$ represents the actuator fault that is estimated in this approach. $\boldsymbol{A}$, $\boldsymbol{B}$, $\boldsymbol{C}$, $\boldsymbol{D}_1$, $\boldsymbol{D}_2$ and $\boldsymbol{R}$ are known as the constant matrices of appropriate dimensions.

The following standard assumptions are introduced to keep the generality of the linear system described above.

Assumption 1. ($\boldsymbol{C}$, $\boldsymbol{A}$) is observable, and $\boldsymbol{A}$ is a Hurwitz matrix.

Assumption 2. ($\boldsymbol{B}$, $\boldsymbol{A}$) is controllable.

Assumption 3. The actuator fault $\boldsymbol{f}(t)$ is the 1-th time derivative, that is, $\dot{\boldsymbol{f}}(t)$, and is assumed to be bounded at the range of the fault occurring time.

Remark 1. Assumptions 1 and 2 are general in most control system designs, and it is worth noting that the supremum of the external disturbances is denoted as $\lambda_0 = \sup_{t\in[0,T]}\|\boldsymbol{d}(t)\|$ in most papers; λ_0 is the constant selected without the theory basis. However, whether the selected λ_0 affects the system deserves further study. Research results will be given in the next section. Fortunately, there are large classes of faults in real composed in Assumption 3.

Definition 1. X is defined as the Banach space, and we denote $\{T(t), t \geq 0\}$ as the bounded linear operator family X→X. The following conditions exist to ensure that $\{T(t), t \geq 0\}$ is a bounded linear operator semigroup. If the following equations hold:

① $T(0) = \boldsymbol{I}$;

② $T(t+s) = T(t)T(s) = T(s)T(t) \quad (t, s \geq 0)$;

③ $\lim_{t\to 0^+}\|T(t)x - x\| = 0$, $x \in X$;

Definition 2. The AFTCS for systems (1) and (2) is to design AFTC law $\boldsymbol{u} = \hat{\boldsymbol{u}}(\boldsymbol{x}(t), \boldsymbol{f}(t))$ such that for $\forall \boldsymbol{x}(0) \in \Re^n$ and $\forall \boldsymbol{f}(t) \in \mathcal{F}$, the trajectory of the system (1) is bounded for $\forall t \geq 0$.

Lemma 1. $\partial_1(t)$, $\partial_2(t)$, $\partial_3(t)$ denote as positive semi-define continuous formula, if there exists

$\partial_0 \in R^+$ such that

$$\partial_1(t) \le \partial_0 + \int_0^t [\partial_2(\tau)\partial_1(\tau) + \partial_3(\tau)]d\tau$$

and then： $\partial_1(t) \le \partial_0 \exp[\int_0^t [\partial_2(\tau) + \partial_3(\tau)/\partial_0]d\tau]$

The main purpose of this paper is to construct a generalized fault diagnosis observer that can estimate the states and fault simultaneously. Subsequently, we propose an active adaptive state feedback controller that resorts to fault estimation information, which can result in the system with actuator faults in a stable condition. The whole scheme of the proposed algorithm is depicted as follows:

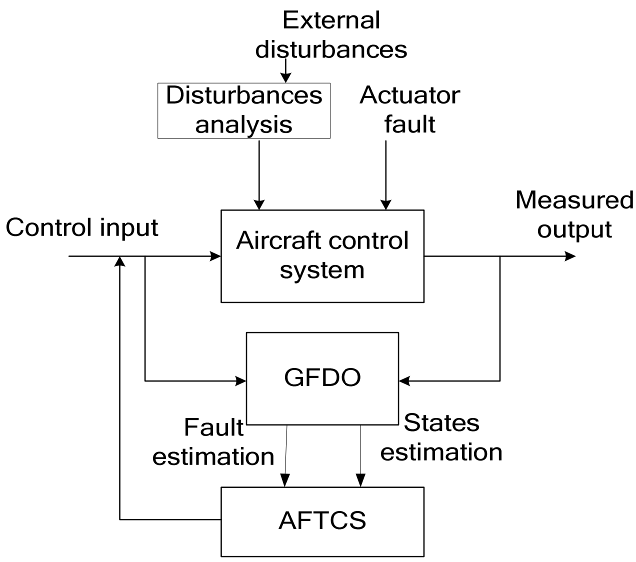

Figure 1. Block diagram of the proposed algorithm.

3. Stability analysis and derivation of the external disturbances constraint condition

Generally, it is impractical to model the external disturbances accurately because of the universal existence of model uncertainties in real applications. At present, scholars deal with external disturbances assuming that they are norm bounded in general, as described above. However, the constraint condition of external disturbances plays a key role in system stability. Unfortunately, few papers examine the issues under the fault diagnosis background. A novel constraint condition of external disturbances that can satisfy the system stability is derived in this section.

Theorem 1. Consider systems (1) and (2) with external disturbances and actuator faults. There exist $M \ge 1, \omega < 0, t \ge 0$ such that the system holds stable globally. As a result, the constraint condition of external disturbances satisfies the inequality as follows:

$$\|\boldsymbol{\upsilon}(\tau)\| < \frac{\|M\boldsymbol{B}\boldsymbol{u}(\tau)\| - \omega\|\boldsymbol{x}(\tau)\|}{\|M\boldsymbol{R}_0\|}$$

with definition $\boldsymbol{R}_0 = [\boldsymbol{D}_1 \quad \boldsymbol{R}]$, $\boldsymbol{\upsilon}(\tau) = \begin{bmatrix} \boldsymbol{d}(\tau) \\ \boldsymbol{f}(\tau) \end{bmatrix}$.

Proof. It is straightforward to obtain that matrix $\boldsymbol{A}$ can derive an operator set, and then the set can generate an asymptotically convergent linear semigroup ζ_t from Assumption 1 and Definition 1 for the state-space description systems (1) and (2). Consequently, there exist $M \geq 1$, $\omega < 0$, $t \geq 0$ such that ζ_t satisfies:

$$\|\zeta_t\| \leq M \exp(\omega t) \tag{3}$$

The trajectory of systems (1) and (2) is represented as:

$$\boldsymbol{x}(t) = \boldsymbol{x}_0 + \int_0^t [\boldsymbol{A}\boldsymbol{x}(\tau) + \boldsymbol{B}\boldsymbol{u}(\tau) + \boldsymbol{D}_1\boldsymbol{d}(\tau) + \boldsymbol{R}\boldsymbol{f}(\tau)]d\tau \tag{4}$$

Then, there exists a stable linear semigroup ζ_t such that Formula (4) can be rewritten as:

$$\boldsymbol{x}(t) = \zeta_t\boldsymbol{x}(0) + \zeta_{t-\tau}\int_0^t [\boldsymbol{B}\boldsymbol{u}(\tau) + \boldsymbol{D}_1\boldsymbol{d}(\tau) + \boldsymbol{R}\boldsymbol{f}(\tau)]d\tau \tag{5}$$

Modelled the 2-norm form for each side of (5)

$$\|\boldsymbol{x}(t)\| = \left\|\zeta_t\boldsymbol{x}(0) + \zeta_{t-\tau}\int_0^t [\boldsymbol{B}\boldsymbol{u}(\tau) + \boldsymbol{D}_1\boldsymbol{d}(\tau) + \boldsymbol{R}\boldsymbol{f}(\tau)]d\tau\right\| \tag{6}$$

It follows with definition $\|\boldsymbol{x}(0)\| = a$

$$\|\boldsymbol{x}(t)\| \leq \|\zeta_t\boldsymbol{x}(0)\| + \left\|\zeta_{t-\tau}\int_0^t [\boldsymbol{B}\boldsymbol{u}(\tau) + \boldsymbol{D}_1\boldsymbol{d}(\tau) + \boldsymbol{R}\boldsymbol{f}(\tau)]d\tau\right\|$$

$$\|\boldsymbol{x}(t)\| \leq Ma\exp(\omega t) + \int_0^t \|M\exp[\omega(t-\tau)][\boldsymbol{B}\boldsymbol{u}(\tau) + \boldsymbol{R}_0\boldsymbol{\upsilon}(\tau)]\|d\tau$$

$$\|\boldsymbol{x}(t)\|\exp(-\omega t) \leq Ma + \int_0^t \frac{\|\boldsymbol{x}(\tau)\|\exp(-\omega\tau)\|M[\boldsymbol{B}\boldsymbol{u}(\tau) + \boldsymbol{R}_0\boldsymbol{\upsilon}(\tau)]\|}{\|\boldsymbol{x}(\tau)\|}d\tau$$

Furthermore, we can obtain from Lemma 1

$$\|\boldsymbol{x}(t)\|\exp(-\omega t) \leq Ma\exp\{\int_0^t \frac{\|M[\boldsymbol{B}\boldsymbol{u}(\tau) + \boldsymbol{R}_0\boldsymbol{\upsilon}(\tau)]\|}{\|\boldsymbol{x}(\tau)\|}d\tau\}$$

$$\|\boldsymbol{x}(t)\| \leq Ma\exp\{\int_0^t \left[\omega + \frac{\|M[\boldsymbol{B}\boldsymbol{u}(\tau) + \boldsymbol{R}_0\boldsymbol{\upsilon}(\tau)]\|}{\|\boldsymbol{x}(\tau)\|}\right]d\tau\}$$

If the system with external disturbances and actuator faults asymptotically converges, the following representation should be satisfied:

$$\omega + \frac{\|M[\boldsymbol{B}\boldsymbol{u}(\tau) + \boldsymbol{R}_0\boldsymbol{\upsilon}(\tau)]\|}{\|\boldsymbol{x}(\tau)\|} < 0 \tag{7}$$

Since

$$\|M\boldsymbol{R}_0\boldsymbol{\upsilon}(\tau)\| - \|M\boldsymbol{B}\boldsymbol{u}(\tau)\| < \|M[\boldsymbol{B}\boldsymbol{u}(\tau) + \boldsymbol{R}_0\boldsymbol{\upsilon}(\tau)]\| < -\omega\|\boldsymbol{x}(\tau)\|$$

Therefore, the constraint condition of the external disturbances (including actuator faults) that can satisfy the system asymptotic convergence is represented as

$$\|\boldsymbol{\upsilon}(\tau)\| < \frac{\|M\boldsymbol{B}\boldsymbol{u}(\tau)\| - \omega\|\boldsymbol{x}(\tau)\|}{\|M\boldsymbol{R}_0\|} \tag{8}$$

As a result, we can analyse the system stability by applying Eq (8). This completes the proof.

Remark 2. The system considered in this paper can hold stable under the constraint conditions derived above. Not all the assumed norm bounded conditions result in the system in a stable condition. For example, we denote the constraint condition of external disturbances as in most papers: $\lambda_0 = \sup_{t\in[0,T]} \|\boldsymbol{d}(t)\|$. It is obvious that systems (1) and (2) are unstable when λ_0 is greater than that of the external disturbance supremum. Therefore, the stability analysis method in this paper is constructive for AFTCSs or even systems analysis.

4. Generalized fault diagnosis observer (GFDO) design

This section focuses on the generalized fault diagnosis observer (GFDO) design to estimate the fault and the state simultaneously. Two defined performance indices should be satisfied for the proposed observer.

Consider the observer for systems (1) and (2) as follows:

$$\dot{\hat{\boldsymbol{x}}}(t) = \boldsymbol{A}\hat{\boldsymbol{x}}(t) + \boldsymbol{B}\boldsymbol{u}(t) + \boldsymbol{R}\hat{\boldsymbol{f}}(t) + \boldsymbol{L}\left[\boldsymbol{y}(t) - \hat{\boldsymbol{y}}(t)\right] \tag{9}$$

$$\hat{\boldsymbol{y}}(t) = \boldsymbol{C}\hat{\boldsymbol{x}}(t) \tag{10}$$

where, $\hat{\boldsymbol{x}}(t)$ is an estimate for state $\boldsymbol{x}(t)$, $\hat{\boldsymbol{f}}(t)$ is an estimate for actuator fault $\boldsymbol{f}(t)$, $\boldsymbol{L}$ is the matrix to be designed. Define $\boldsymbol{r}(t) = \boldsymbol{y}(t) - \hat{\boldsymbol{y}}(t)$, $\boldsymbol{e}(t) = \boldsymbol{x}(t) - \hat{\boldsymbol{x}}(t)$ and $\boldsymbol{e}_f(t) = \boldsymbol{f}(t) - \hat{\boldsymbol{f}}(t)$ as the residual, state estimation error and fault estimation error, respectively.

Theorem 2. Consider systems (1) and (2) with the generalized fault diagnosis observer. For the given positive constant scalars ε_0 and σ, if there exist symmetric positive definite matrices $\boldsymbol{P}$ and $\boldsymbol{P}_1$ such that the following conditions are feasible, then there exist $\boldsymbol{R}_1$, $\boldsymbol{R}_2$ and $\boldsymbol{L}$ such that the proposed generalized fault diagnosis observer has progressive convergence with the index definition performance.

$$\begin{bmatrix} -[(\boldsymbol{A}-\boldsymbol{LC})^T\boldsymbol{P}+\boldsymbol{P}(\boldsymbol{A}-\boldsymbol{LC})] & -\boldsymbol{PR} & -\boldsymbol{P}(\boldsymbol{D}_1-\boldsymbol{LD}_2) & \boldsymbol{C}^T \\ -\boldsymbol{R}^T\boldsymbol{P} & -(\boldsymbol{R}_1+\boldsymbol{R}_1^T)-\boldsymbol{R}_2\boldsymbol{R}_2^T & 0 & -\boldsymbol{R}_2 \\ -(\boldsymbol{D}_1-\boldsymbol{LD}_2)^T\boldsymbol{P} & 0 & -\sigma^2\boldsymbol{I} & \boldsymbol{D}_2^T \\ \boldsymbol{C} & -\boldsymbol{R}_2^T & \boldsymbol{D}_2 & -\boldsymbol{I} \end{bmatrix} \le 0$$

$$\begin{bmatrix} -\sigma^2\boldsymbol{I} & -\boldsymbol{R}_1^T & 0 \\ -\boldsymbol{R}_1 & 0 & \boldsymbol{I} \\ 0 & \boldsymbol{I} & -\sigma^2\boldsymbol{I} \end{bmatrix} \le 0$$

$$\lambda_{\max}(\boldsymbol{\Xi}) \le \frac{\varepsilon_0^2}{\|\boldsymbol{\Omega}\|^2}$$

with definition

$$\boldsymbol{\Xi} = \begin{bmatrix} 0 & 0 & -\boldsymbol{C}^T\boldsymbol{R}_2^T\boldsymbol{P}_1 & \boldsymbol{C}^T\boldsymbol{R}_2^T\boldsymbol{P}_1 & 0 \\ 0 & 0 & -\boldsymbol{D}_2^T\boldsymbol{R}_2^T\boldsymbol{P} & \boldsymbol{D}_2^T\boldsymbol{R}_2^T\boldsymbol{P}_1 & 0 \\ -\boldsymbol{P}_1\boldsymbol{R}_2\boldsymbol{C} & -\boldsymbol{P}_1\boldsymbol{R}_2\boldsymbol{D}_2 & I & -I+\boldsymbol{P}_1\boldsymbol{R}_1 & -\boldsymbol{P}_1 \\ \boldsymbol{P}_1\boldsymbol{R}_2\boldsymbol{C} & \boldsymbol{P}_1\boldsymbol{R}_2\boldsymbol{D}_2 & -I+\boldsymbol{R}_1^T\boldsymbol{P}_1 & I-(\boldsymbol{R}_1^T\boldsymbol{P}_1+\boldsymbol{P}_1\boldsymbol{R}_1) & \boldsymbol{P}_1 \\ 0 & 0 & -\boldsymbol{P}_1 & \boldsymbol{P}_1 & 0 \end{bmatrix}$$

Proof. The time derivative of $\boldsymbol{e}(t)$ for $t > 0$ represents as

$$\begin{aligned}\dot{\boldsymbol{e}}(t) &= \dot{\boldsymbol{x}}(t)-\dot{\hat{\boldsymbol{x}}}(t)\\ &= \boldsymbol{Ax}(t)+\boldsymbol{Bu}(t)+\boldsymbol{D}_1\boldsymbol{d}(t)+\boldsymbol{Rf}(t)-\left\{\boldsymbol{A}\hat{\boldsymbol{x}}(t)+\boldsymbol{Bu}(t)+\boldsymbol{R}\hat{\boldsymbol{f}}(t)+\boldsymbol{L}\left[\boldsymbol{y}(t)-\hat{\boldsymbol{y}}(t)\right]\right\}\\ &= (\boldsymbol{A}-\boldsymbol{LC})\boldsymbol{e}(t)+\boldsymbol{Re}_f(t)+(\boldsymbol{D}_1-\boldsymbol{LD}_2)\boldsymbol{d}(t)\end{aligned} \tag{11}$$

Then, $\dot{\boldsymbol{e}}_f(t)$ follows, similar to the matrices $\boldsymbol{R}_1$ $\boldsymbol{R}_2$ and, which are designed further according to the definition $\dot{\hat{\boldsymbol{f}}}(t)=\boldsymbol{R}_1\hat{\boldsymbol{f}}(t)-\boldsymbol{R}_2\boldsymbol{r}(t)$

$$\begin{aligned}\dot{\boldsymbol{e}}_f(t) &= \dot{\boldsymbol{f}}(t)-\dot{\hat{\boldsymbol{f}}}(t)\\ &= \boldsymbol{R}_2\boldsymbol{r}(t)-\boldsymbol{R}_1\hat{\boldsymbol{f}}(t)+\dot{\boldsymbol{f}}(t)\\ &= \boldsymbol{R}_2\boldsymbol{Ce}(t)+\boldsymbol{R}_1\boldsymbol{e}_f(t)+\boldsymbol{R}_2\boldsymbol{D}_2\boldsymbol{d}(t)-\boldsymbol{R}_1\boldsymbol{f}(t)+\dot{\boldsymbol{f}}(t)\end{aligned} \tag{12}$$

Denote $\bar{\boldsymbol{e}}(t)=\begin{bmatrix}\boldsymbol{e}(t)\\ \boldsymbol{e}_f(t)\end{bmatrix}$, $\boldsymbol{\upsilon}_1(t)=\begin{bmatrix}\boldsymbol{d}(t)\\ \boldsymbol{f}(t)\\ \dot{\boldsymbol{f}}(t)\end{bmatrix}$.

Thus, we obtain the following formulas from (11) and (12):

$$\dot{\bar{\boldsymbol{e}}}(t)=\begin{bmatrix}\boldsymbol{A}-\boldsymbol{LC} & \boldsymbol{R}\\ \boldsymbol{R}_2\boldsymbol{C} & \boldsymbol{R}_1\end{bmatrix}\bar{\boldsymbol{e}}(t)+\begin{bmatrix}\boldsymbol{D}_1-\boldsymbol{LD}_2 & 0 & 0\\ \boldsymbol{R}_2\boldsymbol{D}_2 & -\boldsymbol{R}_1 & \boldsymbol{I}\end{bmatrix}\boldsymbol{\upsilon}_1(t) \tag{13}$$

Hence, the residual $\boldsymbol{r}(t)$ follows that

$$\boldsymbol{r}(t)=\begin{bmatrix}\boldsymbol{C} & \boldsymbol{0}\end{bmatrix}\bar{\boldsymbol{e}}(t)+\begin{bmatrix}\boldsymbol{D}_2 & \boldsymbol{0} & \boldsymbol{0}\end{bmatrix}\boldsymbol{\upsilon}_1(t) \tag{14}$$

One performance index for the generalized observer is defined as

$$\|\boldsymbol{r}(t)\|\le\sigma\|\boldsymbol{\upsilon}_1(t)\| \tag{15}$$

where σ is the positive constant.

For the generalized observer system described by (13) and (14), a Lyapunov candidate function is defined as

$$V(t)=\boldsymbol{e}^T(t)\boldsymbol{Pe}(t)+\boldsymbol{e}_f^T(t)\boldsymbol{e}_f(t) \tag{16}$$

In term of (15), we have

$$\int_0^t\left[\boldsymbol{r}^T(\tau)\boldsymbol{r}(\tau)-\sigma^2\boldsymbol{\upsilon}_1^T(\tau)\boldsymbol{\upsilon}_1(\tau)-\dot{V}(\tau)\right]d\tau+V(t)\le 0 \tag{17}$$

The derivative of $V(t)$ can be obtained according to (16)

$$\begin{aligned}\dot{V}(t) &= \dot{\boldsymbol{e}}^T(t)\boldsymbol{Pe}(t)+\boldsymbol{e}^T(t)\boldsymbol{P}\dot{\boldsymbol{e}}(t)+\dot{\boldsymbol{e}}_f^T(t)\boldsymbol{e}_f(t)+\boldsymbol{e}_f^T(t)\dot{\boldsymbol{e}}_f(t)\\ &= \left[(\boldsymbol{A}-\boldsymbol{LC})\boldsymbol{e}(t)+\boldsymbol{Re}_f(t)+(\boldsymbol{D}_1-\boldsymbol{LD}_2)\boldsymbol{d}(t)\right]^T\boldsymbol{Pe}(t)+\boldsymbol{e}^T(t)\boldsymbol{P}\left[(\boldsymbol{A}-\boldsymbol{LC})\boldsymbol{e}(t)+\boldsymbol{Re}_f(t)+(\boldsymbol{D}_1-\boldsymbol{LD}_2)\boldsymbol{d}(t)\right]\\ &\quad+\left[\boldsymbol{R}_2\boldsymbol{Ce}(t)+\boldsymbol{R}_1\boldsymbol{e}_f(t)+\boldsymbol{R}_2\boldsymbol{D}_2\boldsymbol{d}(t)-\boldsymbol{R}_1\boldsymbol{f}(t)+\dot{\boldsymbol{f}}(t)\right]^T\boldsymbol{e}_f(t)+\boldsymbol{e}_f^T(t)\left[\boldsymbol{R}_2\boldsymbol{Ce}(t)+\boldsymbol{R}_1\boldsymbol{e}_f(t)+\boldsymbol{R}_2\boldsymbol{D}_2\boldsymbol{d}(t)-\boldsymbol{R}_1\boldsymbol{f}(t)+\dot{\boldsymbol{f}}(t)\right]\\ &= \boldsymbol{e}^T(t)(\boldsymbol{A}-\boldsymbol{LC})^T\boldsymbol{Pe}(t)+\boldsymbol{e}_f^T(t)\boldsymbol{R}^T\boldsymbol{Pe}(t)+\boldsymbol{d}^T(t)(\boldsymbol{D}_1-\boldsymbol{LD}_2)^T\boldsymbol{Pe}(t)\\ &\quad+\boldsymbol{e}^T(t)\boldsymbol{P}(\boldsymbol{A}-\boldsymbol{LC})\boldsymbol{e}(t)+\boldsymbol{e}^T(t)\boldsymbol{PRe}_f(t)+\boldsymbol{e}^T(t)\boldsymbol{P}(\boldsymbol{D}_1-\boldsymbol{LD}_2)^T\boldsymbol{d}(t)\\ &\quad+\boldsymbol{e}^T(t)\boldsymbol{C}^T\boldsymbol{R}_2^T\boldsymbol{e}_f(t)+\boldsymbol{e}_f^T(t)\boldsymbol{R}_1^T\boldsymbol{e}_f(t)+\boldsymbol{d}^T(t)\boldsymbol{D}_2^T\boldsymbol{R}_2^T\boldsymbol{e}_f(t)-\boldsymbol{f}^T(t)\boldsymbol{R}_1^T\boldsymbol{e}_f(t)+\dot{\boldsymbol{f}}^T(t)\boldsymbol{e}_f(t)\\ &\quad+\boldsymbol{e}_f^T(t)\boldsymbol{R}_2\boldsymbol{Ce}(t)+\boldsymbol{e}_f^T(t)\boldsymbol{R}_1\boldsymbol{e}_f(t)+\boldsymbol{e}_f^T(t)\boldsymbol{R}_2\boldsymbol{D}_2\boldsymbol{d}(t)-\boldsymbol{e}_f^T(t)\boldsymbol{R}_1\boldsymbol{f}(t)+\boldsymbol{e}_f^T(t)\dot{\boldsymbol{f}}(t)\end{aligned}$$

Substitute $\dot{V}(t)$ into (17), and for simplification, we denote the operation result as

$$\int_0^t \left[\xi_1(\tau)+\xi_2(\tau)\right] d\tau + V(t) \le 0 \tag{18}$$

where

$$\xi_1(\tau)=\begin{bmatrix} e^T(\tau) & e_f^T(\tau) & d^T(\tau)\end{bmatrix}\begin{bmatrix} C^T C-[(A-LC)^T P+P(A-LC)] & -(PR+C^T R_2^T) & C^T D_2 - P(D_1-LD_2) \\ -(R^T P+R_2 C) & -(R_1+R_1^T) & -R_2 D_2 \\ D_2^T C-(D_1-LD_2)^T P & -D_2^T R_2^T & D_2^T D_2-\sigma^2 I \end{bmatrix}\begin{bmatrix} e(\tau) \\ e_f(\tau) \\ d(\tau)\end{bmatrix}$$

$$\xi_2(\tau)=\begin{bmatrix} f^T(\tau) & e_f^T(\tau) & \dot{f}^T(\tau)\end{bmatrix}\begin{bmatrix} -\sigma^2 I & -R_1^T & 0 \\ -R_1 & 0 & I \\ 0 & I & -\sigma^2 I\end{bmatrix}\begin{bmatrix} f(\tau) \\ e_f(\tau) \\ \dot{f}(\tau)\end{bmatrix}$$

Therefore, the generalized observer asymptotically converges if $\xi_1(\tau)\le 0$ and $\xi_2(\tau)\le 0$.

By the Schur complement lemma, the proposed observer asymptotically converges when the parameters of the generalized observer satisfy the following constraint conditions:

$$\begin{bmatrix} -[(A-LC)^T P+P(A-LC)] & -PR & -P(D_1-LD_2) & C^T \\ -R^T P & -(R_1+R_1^T)-R_2 R_2^T & 0 & -R_2 \\ -(D_1-LD_2)^T P & 0 & -\sigma^2 I & D_2^T \\ C & -R_2^T & D_2 & -I \end{bmatrix} \le 0 \tag{19}$$

$$\begin{bmatrix} -\sigma^2 I & -R_1^T & 0 \\ -R_1 & 0 & I \\ 0 & I & -\sigma^2 I\end{bmatrix} \le 0 \tag{20}$$

In this paper, we aim to obtain a high-precision fault estimation error. Therefore, another performance index is defined as:

$$\left\| e_f(t) \right\| < \varepsilon_0 \tag{21}$$

where ε_0 is a prior known constant.

Denote the Lyapunov candidate function

$$V_1(t)=e_f^T(t) P_1 e_f(t)$$

Since the performance index (21) can be rewritten as:

$$\int_0^t \left[e_f^T(\tau) e_f(\tau)-\varepsilon_0^2 \right] d\tau = \int_0^t \left[e_f^T(\tau) e_f(\tau)-\varepsilon_0^2-\dot{V}_1(\tau)\right] d\tau + V_1(t) < 0 \tag{22}$$

The time derivative of $V_1(t)$ is:

$$\begin{aligned} \dot{V}_1(t) = {} & \dot{f}^T(t) P_1 f(t) - \hat{f}^T(t) R_1^T P_1 f(t) + e^T(t) C^T R_2^T P_1 f(t) + d^T(t) D_2^T R_2^T P_1 f(t) \\ & - \dot{f}^T(t) P_1 \hat{f}(t) + \hat{f}^T(t) R_1^T P_1 \hat{f}(t) - e^T(t) C^T R_2^T P_1 \hat{f}(t) - d^T(t) D_2^T R_2^T P_1 \hat{f}(t) \\ & + f^T(t) P_1 \dot{f}(t) - f^T(t) P_1 R_1 \hat{f}(t) + f^T(t) P_1 R_2 C e(t) + f^T(t) P_1 R_2 D_2 d(t) \\ & - \hat{f}^T(t) P_1 \dot{f}(t) + \hat{f}^T(t) P_1 R_1 \hat{f}(t) - \hat{f}^T(t) P_1 R_2 C e(t) - \hat{f}^T(t) P_1 R_2 D_2 d(t) \end{aligned}$$

Therefore, if and only if $\Phi = e_f^T(\tau) e_f(\tau) - \varepsilon_0^2 - \dot{V}_1(\tau) < 0$, the inequality (22) holds. For the sake of convenient description, denote $\Omega^T = \begin{bmatrix} e^T(t) & d^T(t) & f^T(t) & \hat{f}^T(t) & \dot{f}^T(t)\end{bmatrix}$ and substitute $\dot{V}_1(t)$ into Φ, it follows that

$$\boldsymbol{\Omega}^T \boldsymbol{\Xi} \boldsymbol{\Omega} \le \varepsilon_0^2 \tag{23}$$

with definition $\boldsymbol{\Xi} = \begin{bmatrix} 0 & 0 & -\boldsymbol{C}^T \boldsymbol{R}_2^T \boldsymbol{P}_1 & \boldsymbol{C}^T \boldsymbol{R}_2^T \boldsymbol{P}_1 & 0 \\ 0 & 0 & -\boldsymbol{D}_2^T \boldsymbol{R}_2^T \boldsymbol{P}_1 & \boldsymbol{D}_2^T \boldsymbol{R}_2^T \boldsymbol{P}_1 & 0 \\ -\boldsymbol{P}_1 \boldsymbol{R}_2 \boldsymbol{C} & -\boldsymbol{P}_1 \boldsymbol{R}_2 \boldsymbol{D}_2 & I & -I + \boldsymbol{P}_1 \boldsymbol{R}_1 & -\boldsymbol{P}_1 \\ \boldsymbol{P}_1 \boldsymbol{R}_2 \boldsymbol{C} & \boldsymbol{P}_1 \boldsymbol{R}_2 \boldsymbol{D}_2 & -I + \boldsymbol{R}_1^T \boldsymbol{P}_1 & I - (\boldsymbol{R}_1^T \boldsymbol{P}_1 + \boldsymbol{P}_1 \boldsymbol{R}_1) & \boldsymbol{P}_1 \\ 0 & 0 & -\boldsymbol{P}_1 & \boldsymbol{P}_1 & 0 \end{bmatrix}$.

Since

$$\lambda_{\min}(\boldsymbol{\Xi}) \|\boldsymbol{\Omega}\|^2 \le \boldsymbol{\Omega}^T \boldsymbol{\Xi} \boldsymbol{\Omega} \le \lambda_{\max}(\boldsymbol{\Xi}) \|\boldsymbol{\Omega}\|^2$$

Hence, it is obvious that Eq (23) holds if $\lambda_{\max}(\boldsymbol{\Xi}) \|\boldsymbol{\Omega}\|^2 \le \varepsilon_0^2$, as a result

$$\lambda_{\max}(\boldsymbol{\Xi}) \le \frac{\varepsilon_0^2}{\|\boldsymbol{\Omega}\|^2} \tag{24}$$

The proposed generalized fault diagnosis observer that meets the index definition performance asymptotically converges with conditions (19), (20) and (24), which completes the proof.

Remark 3. From Theorem 2, we know that unlike the observer at present, the proposed generalized fault diagnosis observer can estimate actuator fault and state simultaneously. In addition, the defined performance index ensures high precision and high performance for the observer. To enlarge the research set of $\boldsymbol{R}_1$, $\boldsymbol{R}_2$ and $\boldsymbol{L}$, selecting the minimum value of $\|\boldsymbol{\Omega}\|^2$ is feasible in real applications. In other words, the minimum value of $\|\boldsymbol{\Omega}\|^2$ is available because the performance requirement for state estimation error is known as a prior. According to Theorem 1, we can obtain the external disturbance information. Therefore, matrices $\boldsymbol{R}_1$, $\boldsymbol{R}_2$ and $\boldsymbol{L}$ are available by Theorems 1 and 2.

5. Active adaptive fault tolerant controller design

In this section, we focus on the active adaptive state feedback fault tolerant controller design. Consider systems (1) and (2), and the AFTC is designed as

$$\boldsymbol{u}(t) = \hat{\boldsymbol{k}}_1(t)\boldsymbol{x}(t) + \boldsymbol{k}_2(t) \tag{25}$$

where $\hat{\boldsymbol{k}}_1(t)$ and $\boldsymbol{k}_2(t)$ are adaptive control laws defined as

$$\dot{\hat{\boldsymbol{k}}}_1(t) = -\boldsymbol{\eta}_1 \boldsymbol{x}(t)\boldsymbol{x}^T(t)\boldsymbol{P}_2\boldsymbol{B} \tag{26}$$

$$\boldsymbol{k}_2(t) = -\frac{(\boldsymbol{x}^T(t)\boldsymbol{P}_2\boldsymbol{B})^T \|\boldsymbol{x}^T(t)\boldsymbol{P}_2\boldsymbol{B}\| \hat{k}_3(t)}{\|\boldsymbol{x}^T(t)\boldsymbol{P}_2\boldsymbol{B}\|^2} \tag{27}$$

$$\dot{\hat{k}}_3(t) = \eta_2 \|\boldsymbol{x}^T(t)\boldsymbol{P}_2\boldsymbol{B}\| \tag{28}$$

where $\boldsymbol{\eta}_1$ and η_2 are the given constant matrix and positive constant, respectively. Denoted as $\tilde{\boldsymbol{k}}_1(t) = \hat{\boldsymbol{k}}_1(t) - \boldsymbol{k}_1$, $\tilde{k}_3(t) = \hat{k}_3(t) - k_3$ and $\boldsymbol{k}_1$, k_3 are unknown constants that will be obtained later. Therefore, the solution set of AFTCS is located in $(\boldsymbol{x}(t), \tilde{\boldsymbol{k}}_1(t), \tilde{k}_3(t))$.

System Model (1) can be rewritten as follows by applying adaptive controller (25):

$$\dot{\boldsymbol{x}}(t) = (\boldsymbol{A} + \boldsymbol{B}\hat{\boldsymbol{k}}_1(t))\boldsymbol{x}(t) + \boldsymbol{B}\boldsymbol{k}_2(t) + \boldsymbol{D}_1\boldsymbol{d}(t) + \boldsymbol{R}\boldsymbol{f}(t) \tag{29}$$

In the following, the controller parameters of the AFTCS are assured by Theorem 3, guaranteeing the system with actuator fault and external disturbances asymptotically convergence.

Theorem 3. Consider the system described as in (29) with the adaptive control laws (25). If there exists a symmetric positive definite matrix $\boldsymbol{P}_2$ and the unknown parameters selected in AFTCS satisfy the constraint conditions (35) and (36), then the proposed active adaptive fault tolerant controller asymptotically converges with the gain matrix (26) to (28).

Proof. Define a Lyapunov candidate function for the system described by (29) as

$$V_2(\boldsymbol{x}(t), \tilde{\boldsymbol{k}}_1(t), \tilde{k}_3(t)) = \boldsymbol{x}^T(t)\boldsymbol{P}_2\boldsymbol{x}(t) + \sum_{i=1}^{2} \tilde{\boldsymbol{k}}_{1,i}^T(t)\boldsymbol{\eta}_1^{-1}\tilde{\boldsymbol{k}}_{1,i}(t) + \eta_2^{-1}\tilde{k}_3^2(t) \tag{30}$$

where, $\dot{\hat{\boldsymbol{k}}}_{1,i}(t) = -\boldsymbol{\eta}_1\boldsymbol{x}(t)\boldsymbol{x}^T(t)\boldsymbol{P}_2\boldsymbol{b}_i$, $\tilde{\boldsymbol{k}}_{1,i}(t) = \hat{\boldsymbol{k}}_{1,i}(t) - \boldsymbol{k}_{1,i}$ and the parameters therein are defined as $\hat{\boldsymbol{k}}_1(t) = \begin{bmatrix} \hat{\boldsymbol{k}}_{1,1}(t) & \hat{\boldsymbol{k}}_{1,2}(t) \end{bmatrix}$, $\hat{\boldsymbol{k}}_{1,1}(t) = \begin{bmatrix} \hat{\boldsymbol{k}}_{11}(t) \\ \hat{\boldsymbol{k}}_{21}(t) \end{bmatrix}$, $\hat{\boldsymbol{k}}_{1,2}(t) = \begin{bmatrix} \hat{\boldsymbol{k}}_{12}(t) \\ \hat{\boldsymbol{k}}_{22}(t) \end{bmatrix}$, $\boldsymbol{k}_1 = \begin{bmatrix} \boldsymbol{k}_{1,1} & \boldsymbol{k}_{1,2} \end{bmatrix}$, $\boldsymbol{k}_{1,1} = \begin{bmatrix} \boldsymbol{k}_{11} \\ \boldsymbol{k}_{21} \end{bmatrix}$, $\boldsymbol{k}_{1,2} = \begin{bmatrix} \boldsymbol{k}_{12} \\ \boldsymbol{k}_{22} \end{bmatrix}$, $\boldsymbol{B} = \begin{bmatrix} \boldsymbol{b}_1 & \boldsymbol{b}_2 \end{bmatrix}$, $\boldsymbol{b}_1 = \begin{bmatrix} b_{11} \\ b_{21} \end{bmatrix}$, $\boldsymbol{b}_2 = \begin{bmatrix} b_{12} \\ b_{22} \end{bmatrix}$.

The time derivate of $V_2(\boldsymbol{x}(t), \tilde{\boldsymbol{k}}_{1,i}(t), \tilde{k}_3(t))$ is

$$\begin{aligned}
\dot{V}_2(\boldsymbol{x}(t), \tilde{\boldsymbol{k}}_1(t), \tilde{k}_3(t)) &= \dot{\boldsymbol{x}}^T(t)\boldsymbol{P}_2\boldsymbol{x}(t) + \boldsymbol{x}^T(t)\boldsymbol{P}_2\dot{\boldsymbol{x}}(t) + \sum_{i=1}^{2}\left[\dot{\tilde{\boldsymbol{k}}}_{1,i}^T(t)\boldsymbol{\eta}_1^{-1}\tilde{\boldsymbol{k}}_{1,i}(t) + \tilde{\boldsymbol{k}}_{1,i}^T(t)\boldsymbol{\eta}_1^{-1}\dot{\tilde{\boldsymbol{k}}}_{1,i}(t)\right] + 2\eta_2^{-1}\tilde{k}_3(t)\dot{\tilde{k}}_3(t) \\
&= \boldsymbol{x}^T(t)\left[(\boldsymbol{A} + \boldsymbol{B}\hat{\boldsymbol{k}}_1(t))^T\boldsymbol{P}_2 + \boldsymbol{P}_2(\boldsymbol{A} + \boldsymbol{B}\hat{\boldsymbol{k}}_1(t))\right]\boldsymbol{x}(t) + 2\boldsymbol{x}^T(t)\boldsymbol{P}_2\boldsymbol{B}\boldsymbol{k}_2(t) + 2\boldsymbol{x}^T(t)\boldsymbol{P}_2\boldsymbol{D}_1\boldsymbol{d}(t) \\
&\quad + 2\boldsymbol{x}^T(t)\boldsymbol{P}_2\boldsymbol{R}\boldsymbol{f}(t) + \Delta_1
\end{aligned}$$

where, for convenient of statement, denote as $\Delta_1 = 2\eta_2^{-1}\tilde{k}_3(t)\dot{\tilde{k}}_3(t) + \sum_{i=1}^{2}\left[\dot{\tilde{\boldsymbol{k}}}_{1,i}^T(t)\boldsymbol{\eta}_1^{-1}\tilde{\boldsymbol{k}}_{1,i}(t) + \tilde{\boldsymbol{k}}_{1,i}^T(t)\boldsymbol{\eta}_1^{-1}\dot{\tilde{\boldsymbol{k}}}_{1,i}(t)\right]$. And Then, according to the updated laws (26)–(28), $\dot{V}_2(\boldsymbol{x}(t), \tilde{\boldsymbol{k}}_1(t), \tilde{k}_3(t))$ follows that

$$\begin{aligned}
\dot{V}_2(\boldsymbol{x}(t), \tilde{\boldsymbol{k}}_1(t), \tilde{k}_3(t)) &\le \boldsymbol{x}^T(t)\left[(\boldsymbol{A} + \boldsymbol{B}\hat{\boldsymbol{k}}_1(t))^T\boldsymbol{P}_2 + \boldsymbol{P}_2(\boldsymbol{A} + \boldsymbol{B}\hat{\boldsymbol{k}}_1(t))\right]\boldsymbol{x}(t) - 2\boldsymbol{x}^T(t)\boldsymbol{P}_2\boldsymbol{B}\left[\frac{(\boldsymbol{x}^T(t)\boldsymbol{P}_2\boldsymbol{B})^T\left\|\boldsymbol{x}^T(t)\boldsymbol{P}_2\boldsymbol{B}\right\|\hat{k}_3(t)}{\left\|\boldsymbol{x}^T(t)\boldsymbol{P}_2\boldsymbol{B}\right\|^2}\right] \\
&\quad + 2\left\|\boldsymbol{x}^T(t)\boldsymbol{P}_2\right\|\left\|\boldsymbol{D}_1\right\|\left\|\boldsymbol{d}(t)\right\| + 2\left\|\boldsymbol{x}^T(t)\boldsymbol{P}_2\right\|\left\|\boldsymbol{R}\right\|\left\|\boldsymbol{f}(t)\right\| + \Delta_1
\end{aligned}$$

where,

$$\begin{aligned}
\Delta_1 &= 2\eta_2^{-1}\tilde{k}_3(t)\dot{\tilde{k}}_3(t) + \sum_{i=1}^{2}\left[\dot{\tilde{\boldsymbol{k}}}_{1,i}^T(t)\boldsymbol{\eta}_1^{-1}\tilde{\boldsymbol{k}}_{1,i}(t) + \tilde{\boldsymbol{k}}_{1,i}^T(t)\boldsymbol{\eta}_1^{-1}\dot{\tilde{\boldsymbol{k}}}_{1,i}(t)\right] \\
&= 2\eta_2^{-1}(\hat{k}_3(t) - k_3)\dot{\hat{k}}_3(t) - 2\sum_{i=1}^{2}\tilde{\boldsymbol{k}}_{1,i}^T(t)\boldsymbol{x}(t)\boldsymbol{x}^T(t)\boldsymbol{P}_2\boldsymbol{b}_i \\
&= 2\hat{k}_3(t)\left\|\boldsymbol{x}^T(t)\boldsymbol{P}_2\boldsymbol{B}\right\| - 2k_3\left\|\boldsymbol{x}^T(t)\boldsymbol{P}_2\boldsymbol{B}\right\| - 2\sum_{i=1}^{2}\tilde{\boldsymbol{k}}_{1,i}^T(t)\boldsymbol{x}(t)\boldsymbol{x}^T(t)\boldsymbol{P}_2\boldsymbol{b}_i
\end{aligned}$$

As a result

$$\begin{aligned}
\dot{V}_2(\boldsymbol{x}(t), \tilde{\boldsymbol{k}}_1(t), \tilde{k}_3(t)) &\le \boldsymbol{x}^T(t)\left[(\boldsymbol{A} + \boldsymbol{B}\hat{\boldsymbol{k}}_1(t))^T\boldsymbol{P}_2 + \boldsymbol{P}_2(\boldsymbol{A} + \boldsymbol{B}\hat{\boldsymbol{k}}_1(t))\right]\boldsymbol{x}(t) + 2\left\|\boldsymbol{x}^T(t)\boldsymbol{P}_2\right\|\left\|\boldsymbol{D}_1\right\|\left\|\boldsymbol{d}(t)\right\| \\
&\quad + 2\left\|\boldsymbol{x}^T(t)\boldsymbol{P}_2\right\|\left\|\boldsymbol{R}\right\|\left\|\boldsymbol{f}(t)\right\| - 2k_3\left\|\boldsymbol{x}^T(t)\boldsymbol{P}_2\boldsymbol{B}\right\| - 2\sum_{i=1}^{2}\tilde{\boldsymbol{k}}_{1,i}^T(t)\boldsymbol{x}(t)\boldsymbol{x}^T(t)\boldsymbol{P}_2\boldsymbol{b}_i
\end{aligned} \tag{31}$$

Equation (31) can be rewritten as

$$\dot{V}_2(\boldsymbol{x}(t),\tilde{\boldsymbol{k}}_1(t),\tilde{k}_3(t)) \le \boldsymbol{x}^T(t)(\boldsymbol{A}^T\boldsymbol{P}_2+\boldsymbol{P}_2\boldsymbol{A})\boldsymbol{x}(t)+2\left\|\boldsymbol{x}^T(t)\boldsymbol{P}_2\right\|\left\|\boldsymbol{D}_1\right\|\left\|\boldsymbol{d}(t)\right\| \\ +2\left\|\boldsymbol{x}^T(t)\boldsymbol{P}_2\right\|\left\|\boldsymbol{R}\right\|\left\|\boldsymbol{f}(t)\right\|-2k_3\left\|\boldsymbol{x}^T(t)\boldsymbol{P}_2\boldsymbol{B}\right\|+2\sum_{i=1}^{2}\boldsymbol{k}_{1,i}^T\boldsymbol{x}(t)\boldsymbol{x}^T(t)\boldsymbol{P}_2\boldsymbol{b}_i \tag{32}$$

Therefore, there exist the following constraint such that $\dot{V}_2(\boldsymbol{x}(t),\tilde{\boldsymbol{k}}_1(t),\tilde{k}_3(t)) \le 0$

$$2\left\|\boldsymbol{x}^T(t)\boldsymbol{P}_2\right\|\left\|\boldsymbol{D}_1\right\|\left\|\boldsymbol{d}(t)\right\|+2\left\|\boldsymbol{x}^T(t)\boldsymbol{P}_2\right\|\left\|\boldsymbol{R}\right\|\left\|\boldsymbol{f}(t)\right\|-2k_3\left\|\boldsymbol{x}^T(t)\boldsymbol{P}_2\boldsymbol{B}\right\|<0 \tag{33}$$

$$\boldsymbol{x}^T(t)(\boldsymbol{A}^T\boldsymbol{P}_2+\boldsymbol{P}_2\boldsymbol{A})\boldsymbol{x}(t)+2\sum_{i=1}^{2}\boldsymbol{k}_{1,i}^T\boldsymbol{x}(t)\boldsymbol{x}^T(t)\boldsymbol{P}_2\boldsymbol{b}_i<0 \tag{34}$$

For constraint condition (33), we can know the value of $\left\|\boldsymbol{d}(t)\right\|$ and fault estimation from Theorems 1 and 2, respectively. For simplification, denote $\pi_1=\left\|\boldsymbol{D}_1\right\|\left\|\boldsymbol{d}(t)\right\|$, $\pi_2=\left\|\boldsymbol{R}\right\|\left\|\boldsymbol{f}(t)\right\|$.
Hence, inequation (33) can be rewritten as

$$k_3>\frac{\pi_1+\pi_2}{\left\|\boldsymbol{B}\right\|} \tag{35}$$

On the other hand,

$$\boldsymbol{x}^T(t)(\boldsymbol{A}^T\boldsymbol{P}_2+\boldsymbol{P}_2\boldsymbol{A})\boldsymbol{x}(t)+2\sum_{i=1}^{2}\boldsymbol{k}_{1,i}^T\boldsymbol{x}(t)\boldsymbol{x}^T(t)\boldsymbol{P}_2\boldsymbol{b}_i \le \lambda_{\max}(\boldsymbol{A}^T\boldsymbol{P}_2+\boldsymbol{P}_2\boldsymbol{A})\left\|\boldsymbol{x}(t)\right\|^2+2\left\|\boldsymbol{k}_1\right\|\left\|\boldsymbol{P}_2\boldsymbol{B}\right\|\left\|\boldsymbol{x}(t)\right\|^2$$

Therefore, inequation (34) follows if the unknown constant $\boldsymbol{k}_1$ satisfies

$$\left\|\boldsymbol{k}_1\right\|<\frac{\lambda_{\min}(\boldsymbol{A}^T\boldsymbol{P}_2+\boldsymbol{P}_2\boldsymbol{A})}{2\left\|\boldsymbol{P}_2\boldsymbol{B}\right\|} \tag{36}$$

As a result, the AFTCS with the updated laws (25) to (28) and unknown constant constraint conditions (35) and (36) guarantees that the system asymptotically converges under external disturbances and actuator fault interference, which completes the proof.

Remark 4. In contrast to most existing papers [28,29], we sufficiently consider the external disturbance effect on the system. The proposed AFTCS meets the high-performance requirement in the aircraft control system. It is worth noting that information about $\left\|\boldsymbol{d}(t)\right\|$ and $\left\|\boldsymbol{f}(t)\right\|$ is available based on Theorems 1 and 2, and it is involved in π_1 and π_2 for selecting k_3. On the other hand, if we can obtain the fault information from the generalized fault diagnosis observer, then π_2 can be obtained.

6. Results analysis and discussion

The proposed approach has been performed on the F-18 aircraft control system to evaluate the performance of the proposed algorithm. The following sections show the detailed implementations and simulation results.

6.1 Simulation outlines

Considering the system model described as (1) and (2), the corresponding matrices of the longitudinal dynamic equation of the F-18 aircraft motion are as follows [9]:

$$A=\begin{bmatrix}-1.175 & 0.9871\\ -8.458 & -0.8776\end{bmatrix}, B=\begin{bmatrix}-0.194 & -0.03593\\ -19.29 & -3.803\end{bmatrix}, D_1=D_2=\begin{bmatrix}0.1 & 0.2\\ 0.2 & 0.1\end{bmatrix}, C=\begin{bmatrix}1 & 0\\ 0 & 1\end{bmatrix}, R=\begin{bmatrix}0.1 & 0.2\\ 0.2 & 0.1\end{bmatrix}$$

The whole simulation time is $T=100s$. The initial values of the states are $x(0)=[0 \quad 0]^T$. The input control pre-designed is assumed to be $u(t)=[0.6 \quad 0.6]^T$ and the system with the external disturbances $d(t)=[-0.15*\sin(0.6*t) \quad 0.5]^T$. Besides, the system suffers with the actuator fault $f(t)=[f_1(t) \quad f_2(t)]^T$. The actuator fault pattern is chosen as

$$\begin{cases} f_1(t)=0 & t\in T \\ f_2(t)=\begin{cases}0 & t\in[0,30) \\ 0.5*(1-\exp(0.15*(t-30))) & t\in[30,60] \\ 0 & t\in(60,100)\end{cases} \end{cases} \tag{37}$$

As shown in Figure 2, the system states are divergent at the beginning and then asymptotically converge to $\lim_{t\to\infty} x(t)=[-1.286 \quad -2.437]^T$ under the control input. Therefore, we conclude that the system performs well under the control input predesigned in the fault-free case.

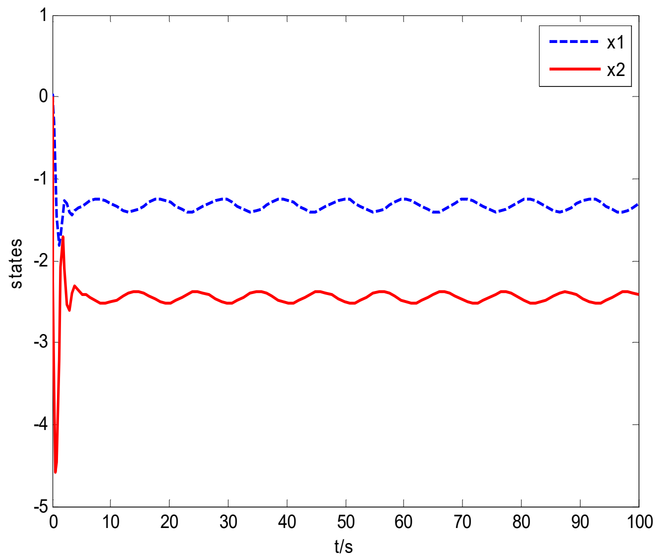

Figure 2. State responses under the fault-free case.

6.2 GFDO simulation

In the GFDO simulation section, the parameters R_1, R_2 and L in Theorem 2 are solved by LMITOOL in MATLAB. Then, the proposed GFDO in Section 4 is implemented by applying the calculated parameters.

We can obtain from (24) that the minimum of $\|\Omega\|$ can enlarge the searching range of R_1, R_2 and L. Therefore, the initial value of Ω is denoted as:

$$\Omega=[0.2 \quad 0.38 \quad -0.15 \quad 0.5 \quad 0 \quad 0.67 \quad 0.49 \quad 0.72 \quad 0.35 \quad 1.75]^T$$

The performance index is defined as σ=1.86, ε_0=2.57. To solve the parameters in (19), (20) and (23), the matrices to be solved are denoted as $P_1*R_2=R_3$, $P_1*R_1=R_4$, $P*L=L_0$. As a result, the parameters are obtained by LMITOOL as follows:

$$\boldsymbol{R}_1 = \begin{bmatrix} -0.4118 & -0.1937 \\ 0.0020 & -0.4316 \end{bmatrix}, \boldsymbol{R}_2 = \begin{bmatrix} 0.2288 & 0.1148 \\ -0.0012 & 0.2405 \end{bmatrix}, \boldsymbol{L} = \begin{bmatrix} 3.0603 & -3.3398 \\ -2.1064 & 5.4404 \end{bmatrix}$$

Subsequently, the GFDO can be applied by the above parameters. Figures 3 and 4 illustrate the state estimation error and fault estimation, respectively. From Figures 3 and 4, we conclude that the desired GFDO results are obtained. Furthermore, Figure 3 shows that the state estimation error asymptotically converges to zero, and the state estimation error increases abruptly because of the fault effect. Figure 4 illustrates that fault estimation can predict the fault signal steadily and accurately. In other words, the GFDO is reliable and effective, as shown in Figures 3 and 4, In conclusion, Table 1 summarizes the mean and standard deviation (std) of the SEE, as well as the desired results. Moreover, Figure 5 shows the state estimation of GFDO compared with the system (1) response under the fault case. Clearly, the fault signal affects the state estimation of GFDO during the fault occurring time $t \in [30, 60]$. Therefore, we can diagnose whether the fault occurs by designing the residual signals. It is straightforward to do so by the proposed GFDO. In this paper, we focus on fault estimation and fault-tolerant controller design. Therefore, the residual design is not stated here. In addition, in real systems, the states are obtained by the designed observer. From Figure 5, we can conclude that the state estimation of the GFDO can track the system state perfectly. Therefore, the simulation results also demonstrate the validity and reliability of the proposed GFDO. It is worth noting that we define the fault pattern as (37) in this simulation. However, the desired fault estimation results are still achieved by the GFDO if the fault pattern is composed in Assumption 3.

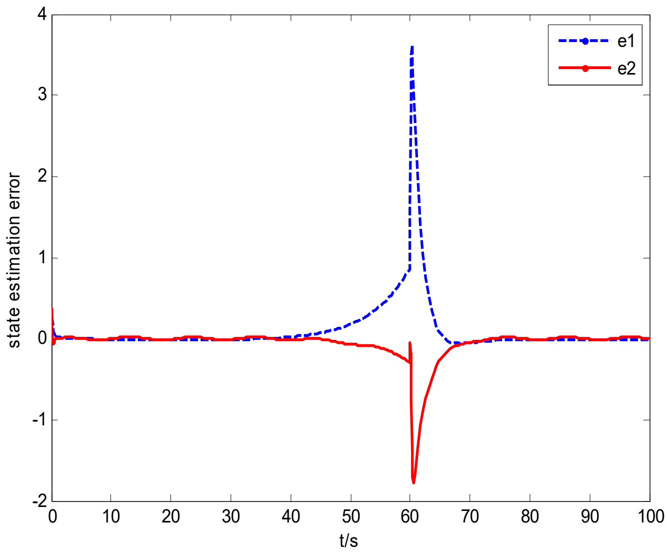

Figure 3. State estimation error.

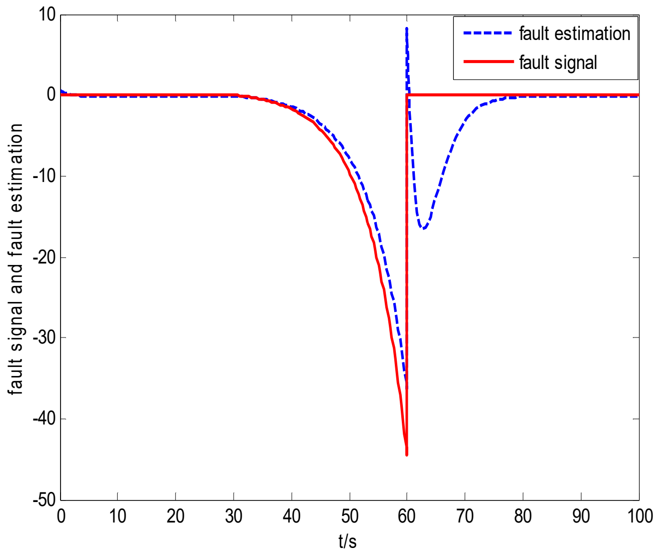

Figure 4. Fault signal and estimation.

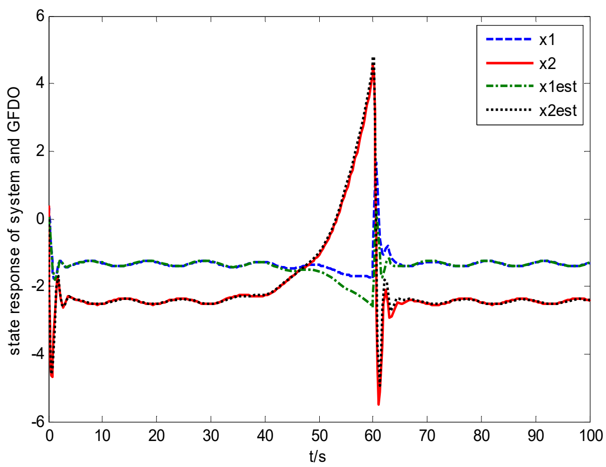

Figure 5. State response of system (1) and GFDO.

Table 1. Statistics character of state estimation error.

	$\boldsymbol{e}_1$	$\boldsymbol{e}_2$
mean	0.2746	-0.1131
std	0.5752	0.2722

6.3 AFTCS implementation

To validate the effectiveness of AFTCS in Section 5, the AFTCS implementation is performed in Simulink. In real systems, when the fault is diagnosed by the proposed GFDO, the normal control law switches to the AFTCS in that obtaining the desired control performance.

To verify the effectiveness of the proposed AFTCS, simulations with the following parameters and initial conditions are given, and the fault and external disturbances are considered in Section 6.2.

$$\eta_1 = 0.00116 * \boldsymbol{I}, \quad \eta_2 = 0.00067, \quad \hat{\boldsymbol{k}}_1(0) = \begin{bmatrix} 0 & 0 \\ 0 & 0 \end{bmatrix}, \quad k_3(0) = 0.79$$

It is necessary to note that the performance of AFTCS is susceptible to the choice of the selected parameters η_1 and η_2. Therefore, to obtain the desired performance, we should choose reasonable values for these parameters in real applications.

Figures 6–8 are the estimated curves of controller parameters $\hat{\boldsymbol{k}}_1(t)$, $\boldsymbol{k}_2(t)$ and $k_3(t)$, respectively. In addition, Figure 9 shows the control law of AFTCSs. Furthermore, Figure 10 and Table 2 show that the desired performance is obtained by the designed AFTCS. In addition, Figure 10 shows the comparison results of the state response between AFTCS and the system with normal control law $\boldsymbol{u}(t) = [0.6 \quad 0.6]^T$. Figure 10 demonstrates that the state curves shock sharply under the normal controller during the outage, and from the state curves of AFTCS, it is clear that the states asymptotically converge. In comparison with the normal controller, the AFTCS shows a better state response, which means the states hold steady compared with the normal controller during the outage. Clearly, the state statistic characters under the normal control and AFTCS are concluded in Table 2, which also demonstrates the effectiveness and superiority of the proposed AFTCS.

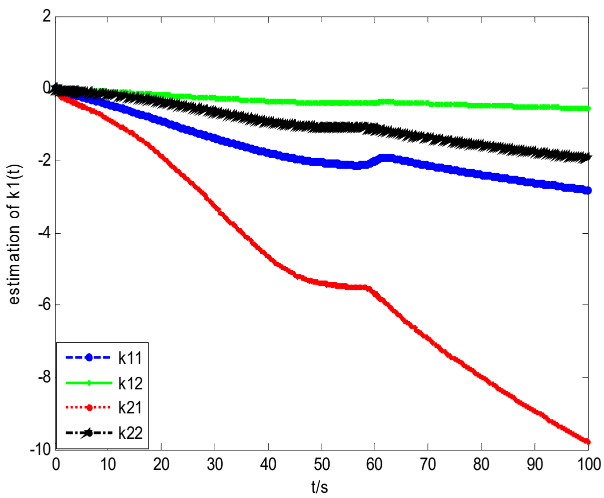

Figure 6. Estimation of $\hat{\boldsymbol{k}}_1(t)$.

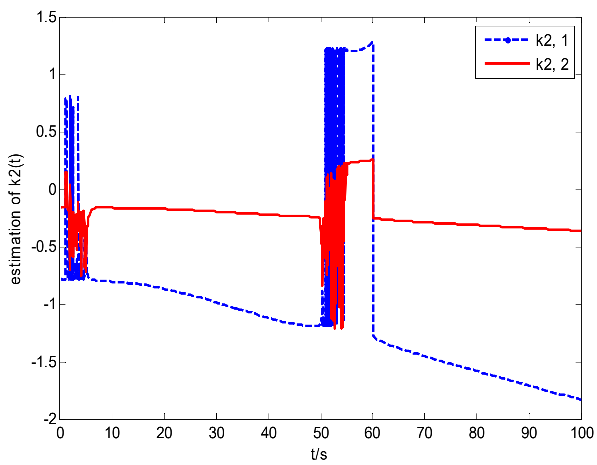

Figure 7. Estimation of $\boldsymbol{k}_2(t)$.

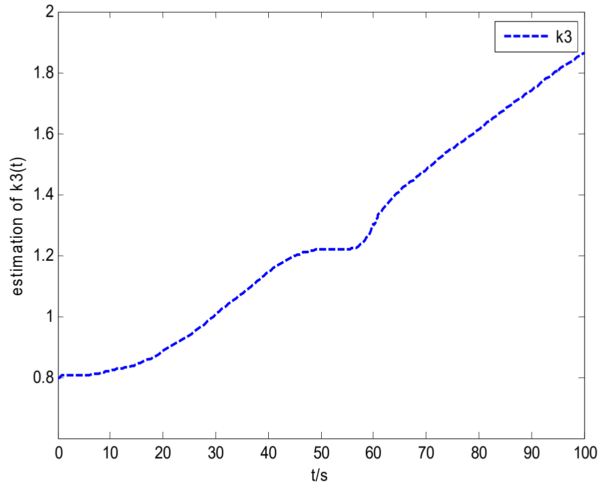

Figure 8. Estimation of $k_3(t)$.

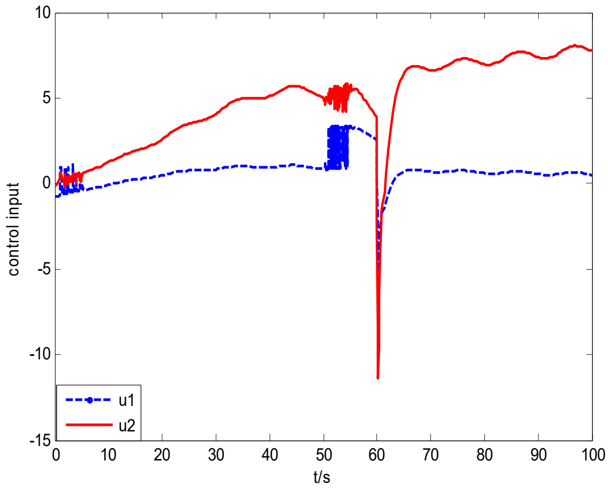

Figure 9. Control input of AFTCS.

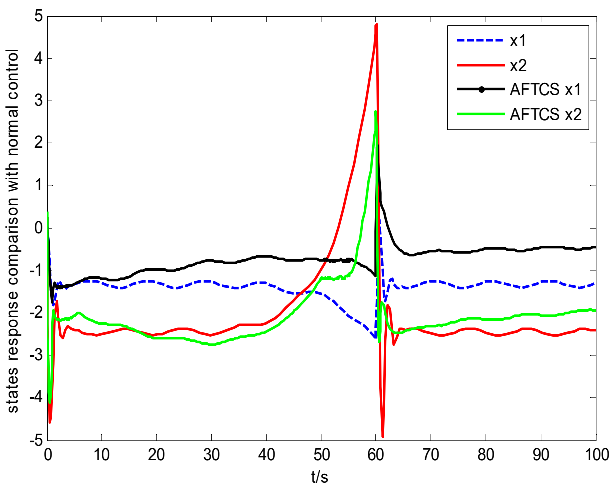

Figure 10. State response comparison between normal control and AFTCS.

Table 2. State statistics character under the normal control AFTCS.

	x_1	x_2	*AFTCS_*x_1	*AFTCS_*x_2
mean	-1.313	-1.809	-0.8305	-1.434
std	0.4867	1.694	0.4268	1.271

7. Conclusions

In this paper, the novel external disturbance constraint condition that satisfies the system stability is derived. Some systems are not stable with the norm bounded assumption. Therefore, the algorithm in Section 3 is meaningful for external disturbance analysis. Then, the GFDO and AFTCS algorithms are proposed. The simulation results show the effectiveness and superiority of the proposed algorithm. In the implementation of GFDO, the desired fault and state estimation performance are obtained. In addition, the states are severely impacted by the normal controller during the outage. However, when the fault is diagnosed and switched to AFTCS, then the system states asymptotically converge and obtain the desired performance. In future work, the proposed algorithm GFDO and AFTCS will be tested with other simulated parameters, and the GFDO will be tested with experimental datasets.

Acknowledgments

The authors thank the guest editor and reviewers for their valuable comments and suggestions which have contributed to improve the presentation of the paper. This work was partially supported by the National Natural Science Foundation of China under Grant 51209049 and the Natural Science Foundation of Heilongjiang Province under Grant LH2021E043.

Conflict of interest

All authors declare no conflicts of interest in this paper.

References

1. Y. Shen, X. Bing, S. X. Ding, D. Zhou, A review on recent development of spacecraft attitude fault tolerant control system, *IEEE Trans. Ind. Electron.*, **63** (2016), 3311–3320. https://doi.org/10.3390/electronics9091513
2. J. H. Fan, Z. Q. Zheng, Y. M. Zhang, Robust fault-tolerant control against time-varying actuator faults and saturation, *IET Control Theory A.*, **6** (2012), 2198–2208. https://doi.org/10.1049/iet-cta.2011.0713
3. A. Abbaspour, S. Mokhtari, A. Sargolzaei, K. K. Yen, A survey on active fault-tolerant control systems, *Electronics-Switz*, **9** (2020), 1513. https://doi.org/10.3390/electronics9091513
4. M. Blanke, M. Staroswiecki, N. E. Wu, Concepts and methods in fault-tolerant control, in *Proceedings of the 2001 American control conference*, 2001. https://doi.org/10.1109/ACC.2001.946264
5. T. V. Costa, R. R. Sencio, L. C. Oliveira-Lopes, F. V. Silva, Fault-tolerant control by means of moving horizon virtual actuators: Concepts and experimental investigation, *Control Eng. Pract.*, **107** (2021), 104683. https://doi.org/10.1016/j.conengprac.2020.104683

6. P. Li, X. Yu, J. Ma, Z. Zheng, Fault-tolerant flight control for an air-breathing hypersonic vehicle using multivariable sliding mode and neural network, in *2017 IEEE 36th Chinese Control Conference (CCC)*, 2017. https:// doi.org/10.23919/ChiCC.2017.8028500
7. Z. Mao, B. Jiang, P. Shi, Fault-tolerant control for a class of nonlinear sampled-data systems via a Euler approximate observer, *Automatica.*, **46** (2010), 1852–1859. https://doi.org/10.1016/j.automatica.2010.06.052
8. P. H. V. Rezende, R. R. Sencio, T. V. Costa, Fault-tolerant control and interval operability for non-square faulty systems, *Braz. J. Chem. Eng.*, **38** (2021), 763–775. https://doi.org/10.1007/s43153-021-00149-8
9. T. Çimen, M. U. Salamci, Flight dynamics, simulation and control with matlab and simulink, in *Workshop at the 20th World Congress of the International Federation of Automatic Control (IFAC WC)*, 2017.
10. M. J. Khosrowjerdi, R. Nikoukhah, N. Safari-Shad, A mixed H2/H∞ approach to simultaneous fault detection and control, *Automatica*, **40** (2004), 261–267. https://doi.org/10.1016/j.automatica.2003.09.011
11. W. Guan, G. Yang, Adaptive fault-tolerant control of linear systems with actuator saturation and L 2-disturbances, *J. Control Theory. Appl.*, **7** (2009), 119–126. https://doi.org/10.1007/s11768-009-8009-2
12. Q. Hu, Robust adaptive sliding-mode fault-tolerant control with L2-gain performance for flexible spacecraft using redundant reaction wheels, *IET Control Theory A.*, **4** (2010), 1055–1070. https://doi.org/10.1049/iet-cta.2009.0140
13. P. A. Luppi, L. Braccia, M. Patrone, D. Zumoffen, Control allocation based fault-tolerant strategy for a bio-ethanol processor system integrated to a PEM fuel cell, *J. Process. Contr.*, **81** (2019), 40–53. https://doi.org/10.1016/j.jprocont.2019.05.021
14. L. F. Mendonça, J. Sousa, J. S. D. Costa, Fault tolerant control using a fuzzy predictive approach, *Expert Syst. Appl.*, **39** (2012), 10630–10638. https://doi.org/10.1016/j.eswa.2012.02.094
15. J. Wang, J. Zhang, Active fault-tolerant control research of multi-agent system, in *Journal of Physics: Conference Series*, 2021. https://doi.org/10.1088/1742-6596/1754/1/012088
16. Z Wang, H Xue, Y Pan, H Liang, Adaptive neural networks event-triggered fault-tolerant consensus control for a class of nonlinear multi-agent systems, *Aims Math.*, **5** (2020), 2780–2800. https://doi.org/10.3934/math.2020179
17. H. Hu, B. Wang, Z. Cheng, L. Liu, Y. Wang, X. Luo, A novel active fault-tolerant control for spacecrafts with full state constraints and input saturation, *Aerosp. Sci. Technol.*, **108** (2021), 106368. https://doi.org/10.1016/j.ast.2020.106368
18. R. Escobar, C. Astorga-Zaragoza, A. Téllez-Anguiano, D. Juárez-Romero, J. Hernández, G. Guerrero-Ramírez, Sensor fault detection and isolation via high-gain observers: Application to a double-pipe heat exchanger, *ISA T.*, **50** (2011), 480–486. https://doi.org/10.1016/j.isatra.2011.03.002
19. J. Stephan, W. Fichter, Gain-scheduled multivariable flight control under uncertain trim conditions, in *2018 AIAA Guidance, Navigation, and Control Conference*, (2018), 1130. https://doi.org/10.2514/6.2018-1130
20. J. Xu, K. Y. Lum, A. P. Loh, A gain-varying UIO approach with adaptive threshold for FDI of nonlinear F16 systems, *J. Control Theory Appl.*, **8** (2010), 317–325. https://doi.org/10.1007/s11768-010-0021-z
21. R. J. Adams, J. M. Buffington, A. G. Sparks, S. S. Banda, Robust multivariable flight control, *Springer Sci. Bus. Media.*, 2012. https://doi.org/10.1007/978-1-4471-2111-4

22. M. Benosman, K. Y. Lum, Application of absolute stability theory to robust control against loss of actuator effectiveness, *IET Control Theory A.*, **3** (2009), 772–788. https://doi.org/10.1049/iet-cta.2008.0216
23. S. Panza, M. Lovera, Rotor state feedback in helicopter flight control: robustness and fault tolerance, in *2014 IEEE Conference on Control Applications (CCA)*, (2014), 451–456. https://doi.org/10.1109/CCA.2014.6981387
24. H. Li, H-infinity bipartite consensus of multi-agent systems with external disturbance and probabilistic actuator faults in signed networks, *AIMS Math.*, **7** (2022), 2019–2043. https://doi.org/10.3934/math.2022116
25. P. Yang, Z. Liu, D. Li, Z. Zhang, Z. Wang, Sliding mode predictive active fault-tolerant control method for discrete multi-faults system, *Int. J. Control Autom.*, **19** (2021), 1228–1240. https://doi.org/10.1007/s12555-020-0046-0
26. W. Chen, M. Saif, A sliding mode observer-based strategy for fault detection, isolation, and estimation in a class of Lipschitz nonlinear systems, *Int. J. Syst. Sci.*, **38** (2007), 943–955. https://doi.org/10.1080/00207720701631503
27. Y. Zhang, Actuator fault-tolerant control for discrete systems with strong uncertainties, *Comput. Chem. Eng.*, **33** (2009), 1870–1878. https://doi.org/10.1016/j.compchemeng.2009.04.004
28. P. Li, J. Ma, Z. Zheng, Robust adaptive multivariable higher-order sliding mode flight control for air-breathing hypersonic vehicle with actuator failures, *Int. J. Adv. Robot. Syst.*, **13** (2016), 1–12. https://doi.org/10.1177/1729881416663376
29. Y. Ding, Y. Wang, S. Jiang, B. Chen, Active fault-tolerant control scheme of aerial manipulators with actuator faults, *J. Cent. South Univ.*, **28** (2021), 771–783. https://doi.org/10.1007/s11771-021-4644-7
30. X. Zhang, L. Liu, Y. Liu, Adaptive NN control based on Butterworth low-pass filter for quarter active suspension systems with actuator failure, *AIMS Math.*, **6** (2021), 754–771. https://doi.org/10.3934/math.2021046
31. F. Zhu, F. Cen, Full-order observer-based actuator fault detection and reduced-order observer-based fault reconstruction for a class of uncertain nonlinear systems, *J. Process. Contr.*, **20** (2010), 1141–1149. https://doi.org/10.1016/j.jprocont.2010.06.021
32. D. Fragkoulis, G. Roux, B. Dahhou, Detection, isolation and identification of multiple actuator and sensor faults in nonlinear dynamic systems: Application to a waste water treatment process, *Appl. Math. Model.*, **35** (2011), 522–543. https://doi.org/10.1016/j.apm.2010.07.019
33. D. Belkhiat, N. Messai, N. Manamanni, Design of a robust fault detection based observer for linear switched systems with external disturbances, *Nonlinear Anal. Hybri.*, **5** (2011), 206–219. https://doi.org/10.1016/j.nahs.2010.10.009
34. M. Khosrowjerdi, Mixed H2/H∞ approach to fault-tolerant controller design for Lipschitz non-linear systems, *IET Control Theory A.*, **5** (2011), 299–307. https://doi.org/10.1049/iet-cta.2009.0556
35. C. Z. Ming-Yue, H. P. Liu, Z. J. Li, D. H. Sun, Fault tolerant control for networked control systems with access constraints, *Acta Autom. Sinica.*, **38** (2012), 1119–1126. https://doi.org/10.1016/S1874-1029(11)60286-3